Theor Chim Acta (1991) 80: 469–482

**Theoretica Chimica Acta**

# Multireference coupled cluster theory in Fock space

## with an application to *s*-tetrazine

**C. M. L. Rittby[1] and R. J. Bartlett[2]**

[1] Department of Physics, Texas Christian University, P.O. Box 32915, Fort Worth, TX 76129, USA

[2] Quantum Theory Project, University of Florida, Williamson Hall, Gainesville, FL 32611, USA

Received February 1, 1991; received in revised form and accepted June 13, 1991

**Summary.** A Fock space multireference coupled cluster method based on incomplete model spaces is described. Some of the essential computational aspects of the theory are discussed with the aid of the diagrammatic representation of the equations. An application to the calculation of ionization potentials and excitation energies of *s*-tetrazine is presented along with comparisons with conventional *ab initio* calculations and experimental results.

**Key words:** Coupled cluster method – Incomplete models spaces – Electronic transition energies

## 1. Introduction

The standard single reference coupled cluster theory has been applied with great success in the calculation of electronic structure of atomic and molecular systems [1–2]. The restriction to a single reference function does, however, put a restriction on the types of states that can be studied. Even though in some cases the inclusion of higher excitations in the wave operator makes it possible to treat quasidegenerate cases in the single reference framework [3] this is not possible for more general multireference cases. Furthermore, even for open shells, the use of unrestricted Hartree–Fock (UHF) reference wavefunctions frequently leads to problems with spin contamination of the final correlated wavefunction. The use of more general reference determinants can be shown to alleviate this problem [4] but a more general coupled cluster theory should, by necessity, be of multireference type.

Multireference coupled cluster theories can be divided into two main categories, Hilbert space [5–8] and Fock space approaches [9–17]. Hilbert space approaches are focused on the description of a system with a fixed number of electrons. The model space is selected so as to include a few dominant configurations in the wavefunction, and the wave-operator and the effective Hamiltonian give information about a few states of the system. Fock space approaches, on the other hand, also attempt to describe the system when the number of electrons is allowed to change, and are geared towards calculating, directly, energy differences such as ionization potentials, excitation energies, and electron affinities between a rather large number of states. The two different approaches are thus complimentary in that they can provide us with different types of information of the system at hand.

The way the model space is constructed is of crucial importance in all multireference approaches. If the particular theory demands the use of a complete model space, where the selected "active" electrons have to occupy all selected "active" orbitals in all possible ways, one is frequently faced with the problem of intruder states. If, in order to circumvent this problem, a theory is constructed to use an incomplete model space one looses some of the potential flexibility inherent in the choice of a larger model space. In what follows we present a Fock space multireference coupled cluster (FSMRCC) method which allows the use of incomplete model spaces [18, 13, 17]. We comment on some of the computational aspects of the approach and we finally present an application to *s*-tetrazine which has been extensively studied with conventional *ab initio* methods.

## 2. Theory

The Fock space multireference coupled cluster theory for incomplete model spaces is based on the existence of a valence-universal wave-operator and the subsystem embedding condition (SEC) [19]. The normal ordered ansatz for the wave-operator [11] leads to a decoupling of model spaces with different particle-hole rank, thus making the method computationally attractive. In the hierarchical solution of the equations, results can thus be used to construct useful intermediates which greatly simplify the iterative solution of the coupled cluster equations.

We start by selecting a closed shell, single determinant wave function $|0\rangle$ (not necessarily Hartree Fock) to which we will refer the holes and particles of our formalism. By creating $m$ particles and $n$ holes from $|0\rangle$ and taking the appropriate linear combinations to satisfy spin-symmetry we form model spaces of different particle-hole rank $(m, n)$ with associated projection operators $P^{(m,n)}$ projecting onto the model space and projection operators $Q^{(m,n)}$ projecting onto the orthogonal complement. Each model space describes a certain type of state in Fock space, e.g., the (0, 1) model space describes singly ionized states and the (1, 1) model space singly excited states.

From a computational point of view we would like to be able to treat only a subset of all possible configurations and we thus divide our orbitals into four categories as shown in Fig. 1. It is usually straightforward to find a natural division for the orbital space but the selection of active and inactive orbital spaces is usually the most common source of subsequent convergence problems in the iterative solution of our equations. At this point it should be made clear that although the model spaces for the (0, 0), (0, 1) and (1, 0) are *complete* since they necessarily include all possible occupancies of electrons among the active orbitals, the (1, 1) model space is *incomplete* since it excludes all doubly, triply etc. excited determinants. The (1, 1) model space is, however, an example of what has been termed a quasicomplete model space [20, 8] in that it is complete with respect to a single vacancy in the active holes and a single occupation in the active particles.

For each $(m, n)$ sector of Fock space our zeroth order wave functions consists of linear combinations of the model space functions:

$$|\Psi_{i0}^{(m,n)}\rangle = \sum_{j=1}^{d} c_{ij}|\phi_j^{(m,n)}\rangle \tag{1}$$

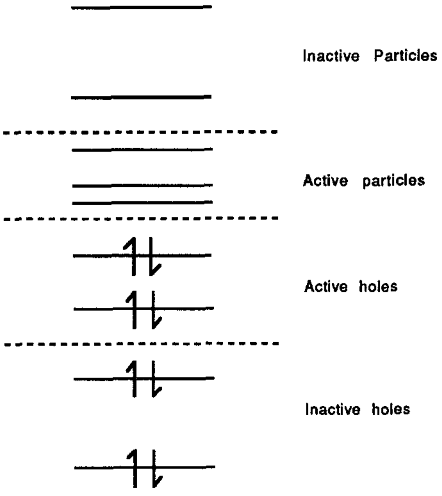

**Fig. 1.** Division of orbital space into active and inactive groups

We introduce a universal wave-operator which takes these model functions into exact solutions of the Schrödinger equation:

$$|\Psi_i^{(m,n)}\rangle = \Omega|\Psi_{i0}^{(m,n)}\rangle \tag{2}$$

It is important to note that here we do not impose intermediate normalization of the wavefunction. It was shown by Mukherjee [18] that such a condition is incompatible with the use of an incomplete model space and in general we have that:

$$P\Omega P \neq P \tag{3}$$

To generate the necessary determinants in the complementary $Q^{(m,n)}$ space we introduce "excitation" and "deexcitation" operators:

$$\begin{aligned} S^{(m,n)} &= \sum_{k=0}^{m} \sum_{l=0}^{n} T^{(k,l)} \\ T^{(k,l)} &= T_1^{(k,l)} + T_2^{(k,l)} + T_3^{(k,l)} + \cdots \end{aligned} \tag{4}$$

where the superscript $(k, l)$ refers to the maximum number of particle $(k)$ and hole $(l)$ destruction operators present and the subscript indicates the excitation or deexcitation level.

Figures 2 and 3 give a graphical representation of the systematic generation of these operators. As perhaps most easily seen in Figs. 2 and 3, unlike ordinary single-reference CC theory, defined by the purely excitation operators, $T^{(0,0)}$; the $T^{(0,1)}$ and $T^{(1,0)}$ operators have "annihilation" lines below the vertex of the diagram. These may be easily understood as corresponding to having one less $(0, 1)$, or one more electron $(1, 0)$. When these operators would act upon the Fermi vacuum $|0\rangle$, they disappear. However, they contribute when applied to the $N-1$ electron model function, $\psi_{i0}^{(0,1)}$ and the $N+1$ electron model function $\psi_{i0}^{(1,0)}$ respectively.

Just as in the single-reference case the series in Eq. (4) has to be truncated at some appropriate level. In terms of the operators in Eq. (4) we now write our ansatz for the universal wave-operator as:

$$\Omega = \{e^S\} \tag{5}$$

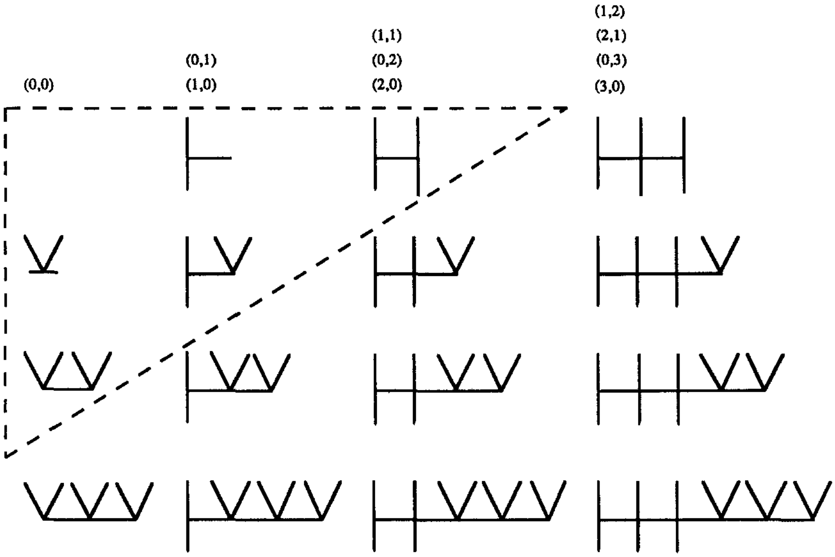

**Fig. 2.** Skeleton "excitation" operators. These operators are formed by adding hole-hole and/or particle-particle scattering lines to the basic excitation operators from the $(0, 0)$ sector. When these additional scattering lines only involve active holes and/or particles the operator is of spectator type. The labels at the top of each column refer to the Fock space sectors where the operators are active. For the first row of diagrams we exclude diagrams giving rise to scattering within the model space

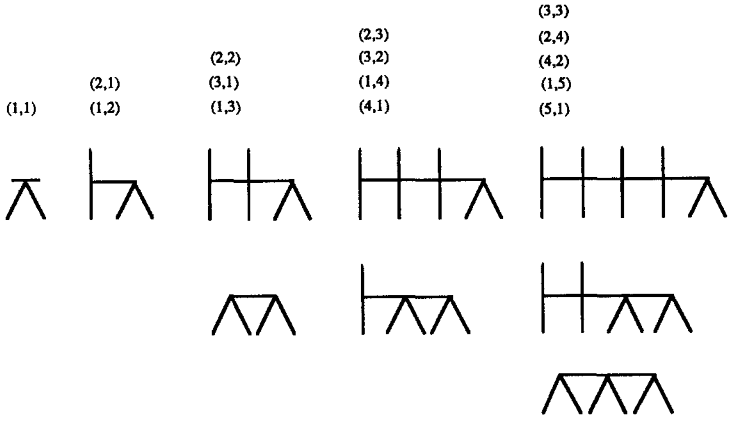

**Fig. 3.** Skeleton "deexcitation" operators. These operators are formed by adding hole-hole and/or particle-particle scattering lines to the basic excitation operators from the $(0, 0)$ sector. When these additional scattering lines only involve active holes and/or particles the operator is of spectator type. The labels at the top of each column refer to the Fock space sectors where the operators are active

where $\{ \}$ denotes normal ordering of the operators with respect to the vacuum state $|0\rangle$. This normal ordering prevents the operators occurring in $S$ to contract amongst themselves and can be shown to lead to a decoupling of the Bloch equations for different sectors:

$$H\Omega P^{(m,n)} - \Omega H_{\text{eff}} P^{(m,n)} = 0 \tag{6}$$

where

$$H_{\mathrm{eff}} = P^{(m,n)}\Omega^{-1}H\Omega P^{(m,n)} \tag{7}$$

is an effective Hamiltonian whose eigenvalues determine the energies of the system and whose eigenvectors give the linear expansion coefficients in Eq. (1).

Introducing normal ordering for the Hamiltonian we get:

$$\begin{aligned}(H_N + \langle 0|H|0\rangle)\Omega P^{(m,n)} - \Omega P^{(m,n)}\Omega^{-1}(H_N + \langle 0|H|0\rangle)\Omega P^{(m,n)} &= 0\\ H_N\Omega P^{(m,n)} - \Omega H_{N,\mathrm{eff}}P^{(m,n)} &= 0\end{aligned} \tag{8}$$

One can further show that this equation holds for connected operators only, i.e.:

$$(H_N\Omega)_c P^{(m,n)} - (\Omega H_{N,\mathrm{eff}})_c P^{(m,n)} = 0 \tag{9}$$

For conceptual as well as for computational reasons it is convenient to define:

$$\tilde{\Omega} = e^{-T}\Omega; \qquad T = S^{(0,0)} \tag{10}$$

and one can easily derive the following Bloch equation from Eq. (8):

$$(\bar{H}_N\tilde{\Omega})_c P^{(m,n)} - (\tilde{\Omega}\bar{H}_{N,\mathrm{eff}})_c P^{(m,n)} = 0 \tag{11}$$

where we have defined a new operator, $H$-bar:

$$\bar{H}_N = (H_N e^T)_{c,\mathrm{open}} \tag{12}$$

and a new effective Hamiltonian:

$$\bar{H}_{N,\mathrm{eff}} = H_{\mathrm{eff}} - (\langle 0|H|0\rangle + (H e^T)_{c,\mathrm{closed}}) = H_{\mathrm{eff}} - E_{\mathrm{CC}} \tag{13}$$

$E_{\mathrm{CC}}$ being the coupled cluster energy of the state defined by the reference function $|0\rangle$. Diagonalizing the effective Hamiltonian in Eq. (13) we directly obtain the energy differences between our states defined by our $(m, n)$ model space and the coupled cluster state defined by our $(0, 0)$ model space function $|0\rangle$.

Equation (11) forms the basis for deriving our working equations in our Fock space method. In what follows we will assume that the $(0, 0)$ sector has been successfully solved and the operator in Eq. (12) has been constructed. In our computational applications we construct the one- and two-body parts of Eq. (12) and store them on disk for subsequent use in other Fock space sectors. We note, however, that the non-hermitean operator of Eq. (12) will have additional contributions of three-body, four-body etc. character.

Let us analyze the equation for the $(0, 1)$ and the $(1, 1)$ sectors in Fock space in more detail. In what follows we will limit ourselves to the CCSD expressions which means that we will restrict our operators in $S^{(m,n)}$ to be of one- and two-body type, i.e., the operators in the dashed triangle of Fig. 2 and the single deexcitation diagram for the $(1, 1)$ sector in Fig. 3. In order to be able to decipher the diagrammatic expression about to be presented, Fig. 4 shows the interpretation of the graphical representations of the operators.

For the calculation of ionization potentials, i.e., the $(0, 1)$ sector, we find from Fig. 2 that two additional operators occur in the wave-operator. The $T_1^{(0,1)}$, operator only occurs if the active hole space is smaller than the full hole space which is, however, generally the case. Note that the new two-body operator includes contributions from operators with a "spectator line", i.e. a single excitation combined with a "null" excitation of an electron in, say orbital $i$, into the same orbital. These operators are important to incorporate relaxation effects

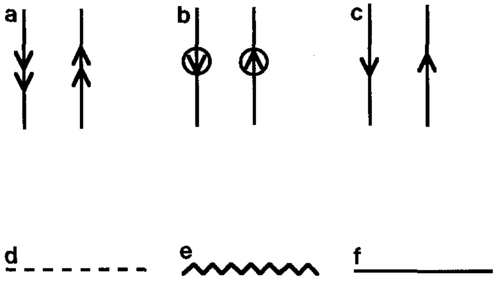

**Fig. 4a–f.** Diagrammatic symbols. Orbital lines are labeled according to the categories in Fig. 1. Active holes and particles are depicted by *double arrows* (**a**), inactive holes and particles by *encircled arrows* (**b**) and when all holes and orbitals are to be included by *plain arrows* (**c**). Hamiltonian interactions are denoted by a *dashed line* (**d**), $H$-bar interaction lines are denoted by a *wavy line* (**e**) and excitations are denoted by *solid lines* (**f**)

in the wavefunction, remembering that we are using the Hartree–Fock orbitals for the ground state to describe all states in Fock space.

Taking the $P^{(0,1)}$ projection of Eq. (11) we can draw the diagrammatic expression for the effective Hamiltonian shown in Fig. 5. The diagonalization of this operator gives us the negative of the ionization potentials defined by the active hole model space functions. Projecting Eq. (11) with the one-body $Q^{(0,1)}$ space we obtain the Fock space coupled cluster equation for the (0, 1) one-body operator shown in Fig. 6. Note the occurrence of the renormalization term (6e) in this equation. The effective Hamiltonian is thus constructed in each step of the iterative solution of the coupled cluster equations and used as an intermediate.

Projecting Eq. (11) with the two-body $Q^{(0,1)}$ space we similarly obtain the Fock space coupled cluster equation for the two-body amplitudes shown in Fig. 7. Again we have a renormalization term, (Fig. 7h), but also a term originating from a three-body contribution to $H$-bar, diagram (Fig. 7g). Since we computationally do not store the three-body terms of $H$-bar such a term has to be calculated "on the fly". This term and its corresponding term for the (1, 0) sector are, however, the only contributing three-body terms in the CCSD approximation which explains the advantage of performing the transformation defined by Eq. (12). Just as for the (0, 0) sector the equations for the (0, 1) amplitudes are coupled and are solved by similar computational techniques. The equations for the (1, 0) sector can be obtained by reversing the direction of all lines in Figs. 5–7.

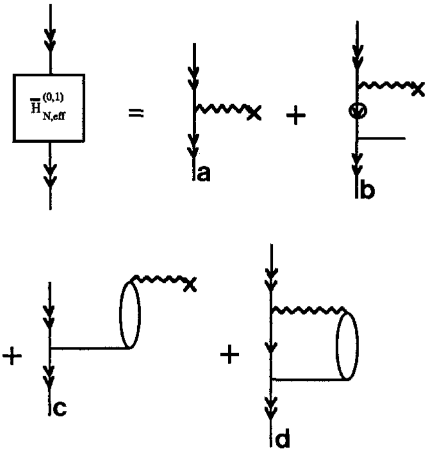

**Fig. 5a–d.** Diagrammatic expressions for the (0, 1) effective Hamiltonian

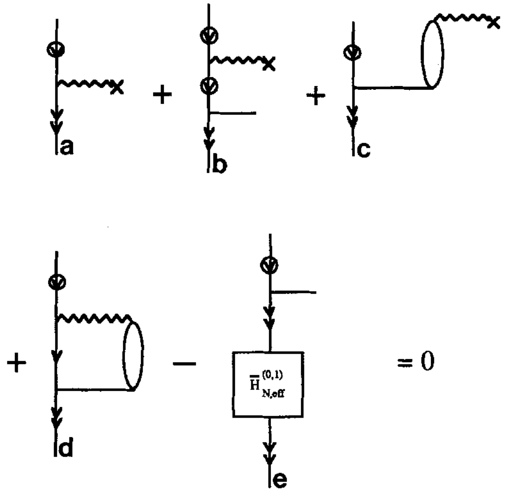

**Fig. 6a–e.** Diagrammatic expression for the $T_1$ amplitudes of the (0, 1) sector

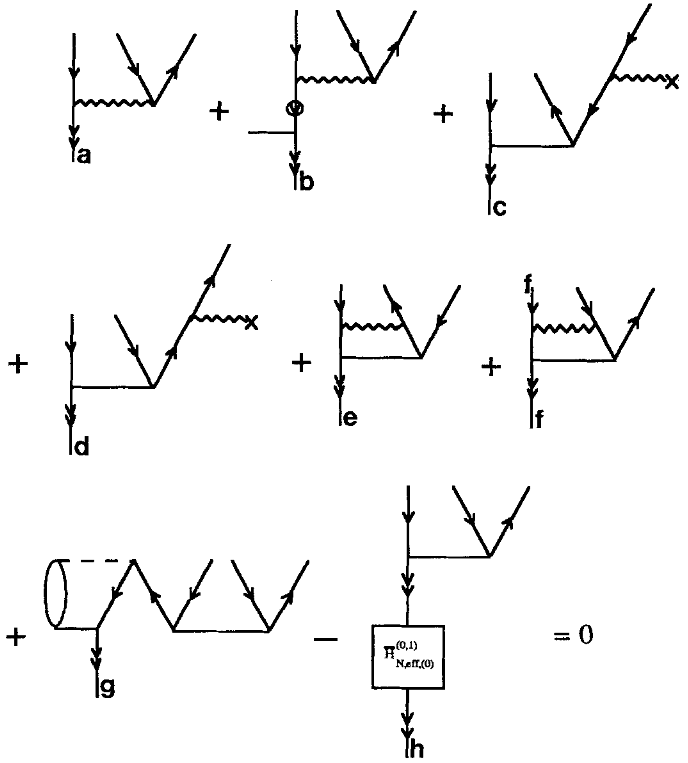

**Fig. 7a–h.** Diagrammatic expression for the $T_2$ amplitudes of the (0, 1) sector

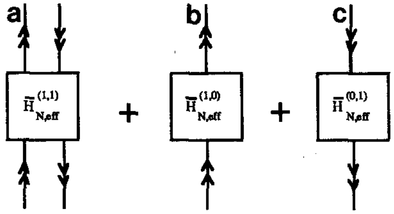

**Fig. 8a–c.** Diagrammatic expression for the effective Hamiltonian for singly excited states

For the (1, 1) sector we again have additional one- and two-body operators contributing to the wave-operator. The new two-body diagram, see Fig. 2, contributes as soon as our active space does not cover all available orbitals. The one-body diagram, see Fig. 3, describes a pure deexcitation to the vacuum state $|0\rangle$, and is, as we shall see, irrelevant for the calculation of the excitation energies.

The $P^{(1,1)}$ projection of the Bloch equation (Eq. (10)) leads to the expression for the effective Hamiltonian shown in Fig. 8. Figures (8b) and (8c) are the effective Hamiltonians determined in the (0, 1) and (1, 0) subsectors.

The equation for the new part of the effective Hamiltonian, diagram Fig. (8a), is given in Fig. 9. Figure (9a) contains contributions from the (0, 0), (0, 1) and (1, 0) subsectors and can therefore be treated as an intermediate with constant amplitudes throughout the evaluation of the (1, 1) sector.

Figures 10 and 11 give the Fock space coupled cluster equation for the $T_1^{(1,1)}$ and $T_2^{(1,1)}$ amplitudes. Again, Figs. (9a) and (10a), contain the contributions from the lower subsectors. Note that there is no coupling between the one- and two-body $T^{(1,1)}$ operators which together with the fact that the effective Hamiltonian is independent of $T_1^{(1,1)}$ (see Fig. 9) means that the excitation energies are not influenced by this one-body operator. The equation defined by Fig. 10 is, however, of very small dimensionality and can easily be solved to obtain the full wave-operator for the (1, 1) sector.

From Figs. 5–11 we find that the subsystem embedding condition gives rise to a rather compact set of equations. The computer code that can be generated from these expressions can therefore be kept fairly transparent and simple by the

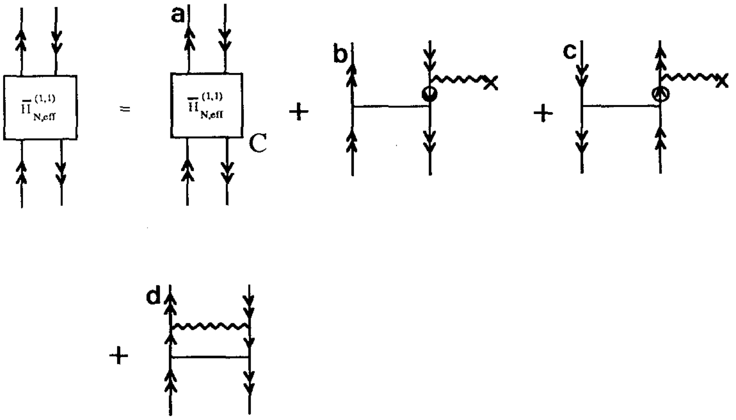

**Fig. 9a–d.** Diagrammatic expression for the (1, 1) effective Hamiltonian

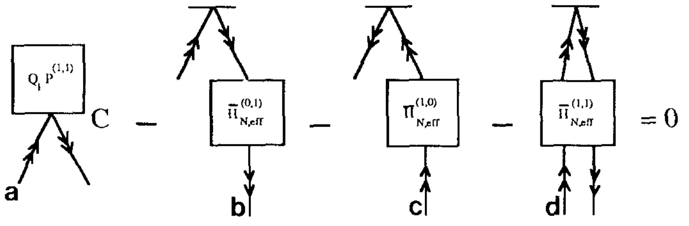

**Fig. 10a–d.** Diagrammatic expression for the $T_1$ amplitudes for the (1, 1) sector. See text for further discussion

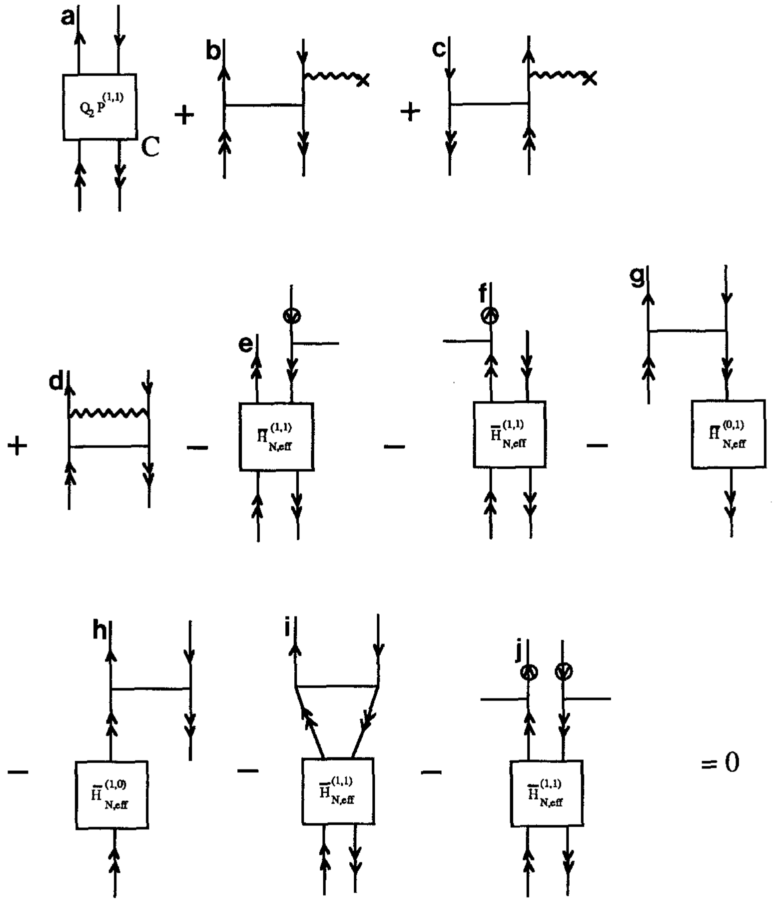

**Fig. 11a–i.** Diagrammatic expression for the $T_2$ amplitudes of the (1, 1) sector. See text for further discussion

construction and storage of relevant intermediate results. Also, the typical computer requirements for FSMRCC calculations are comparable to that for a single reference CC calculation, although it can be more difficult to converge the equations in some cases because of the requirement that several states be described.

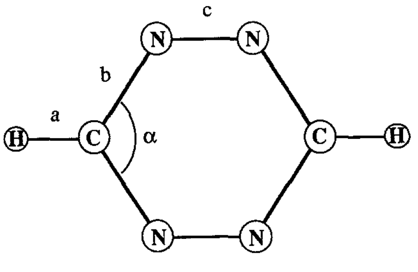

**Fig. 12.** *s*-Tetrazine bond lengths and bond angles. For values of the parameters *a*, *b*, *c*, and α see Table 1

## 3. Application to *s*-tetrazine

We here present some results from an application of the method presented above to *s*-tetrazine (Fig. 12), which has been studied extensively experimentally since the first decades of this century [21, 22]. The *s*-tetrazine molecule has also been the subject of several *ab initio* electronic structure calculations and in Ref. [23] Scheiner and Schaefer presented a thorough review of both the theoretical and experimental status as well as a detailed configuration interaction (CI) study of the excited states for this molecule. Earlier, von Niessen et al. [24] had investigated the photo-electron spectrum of the same system by the use of propagator techniques which together with the work in Ref. [23] gives us a point of comparison for our Fock space calculation. One of the distinguishing features of the present approach is of course that both spectra, along with information concerning electron affinities are obtained in *one* calculation, i.e., in the process of solving for excitation energies we obtain information concerning the other properties from intermediate steps.

The ground state electronic configuration of *s*-tetrazine is given by:

$$1b_{2u}^2\,1a_g^2\,1b_{3g}^2\,1b_{1u}^2\,2a_g^2\,2b_{1u}^2\,3a_g^2\,2b_{2u}^2\,3b_{1u}^2\,2b_{3g}^2\,4a_g^2\,3b_{2u}^2\,5a_g^2\,4b_{1u}^2\,1b_{3u}^2$$

$$4b_{2u}^2\,6a_g^2\,5b_{1u}^2\,1b_{1g}^2\,1b_{2g}^2\,3b_{3g}^2\,1a_u^0\,2b_{3u}^0$$

In our calculations we used the same basis set and geometries (Table 1) as in Ref. [23], i.e., a standard Huzinaga–Dunning DZ basis set [25] augmented with a set cartesian *d*-functions on the carbon and nitrogen atoms with exponents $\alpha_C = 0.75$, $\alpha_N = 0.80$ along with a set of *p*-functions with $\alpha_H = 0.75$ on the hydrogens. We selected the six highest occupied orbitals to be our active hole space and the two lowest virtual orbitals to be our active particle space. Consequently, we will obtain six ionization potentials,

**Table 1.** Geometry from Ref. [23] used in the calculations. For bond lengths and bond angles refer to Fig. 1

| | DZP SCF parameters | Experiment |
|---|---|---|
| *a* | 1.0743 Å | 1.0726 Å |
| *b* | 1.3215 Å | 1.3405 Å |
| *c* | 1.2923 Å | 1.3256 Å |
| α | 125.19° | 126.36° |
| *a* | DZP SCF parameters | Experiment |

**Table 2.** Vertical ionization potentials in eV for *s*-tetrazine (SCF geometry)

| Electronic state | TDA[a] | GF[a] | FSMRCC (DZP) | Experiment |
|---|---|---|---|---|
| $^2B_{3g}$ | 8.91 | 9.24 | 9.20 | 9.7 |
| $^2B_{1u}$ | 11.40 | 11.97 | 11.87 | 11.9 |
| $^2B_{2g}$ | 12.18 | 12.52 | 12.12 | 12.1 |
| $^2A_g$ | 12.21 | 12.64 | 12.69 | 12.8 |
| $^2B_{2u}$ | 12.34 | 12.89 | 13.01 | 13.3 |
| $^2B_{1g}$ | 13.12 | 13.47 | 13.52 | 13.5 |

[a] Ref. [24]

two electron affinities, twelve singlet excitation energies and twelve triplet excitation energies.

Table 2 gives our results for the ionization potentials obtained from the (0, 1) Fock space sector. As is noted in Ref. [24] to make assignments of the photo-electron spectrum for *s*-tetrazine based on Koopmans' theorem "is as useful as looking it up in a telephone directory". A correlated method is necessary in order to even get the correct qualitative description of the spectrum. Our results are in general agreement with the Green's function calculation of von Nissen et al. [24] except for the ionization from the $3b_{2g}$ orbital where the difference is 0.4 eV. The agreement with experiment is also good except for the first ionization potential. Errors up to 0.3 eV might be reasonable, but we seriously doubt if our predicted first IP is in error by 0.5 eV, recommending a reconsideration of the observed ionization threshold.

In order to get the excitation energy spectrum we also solve the (1, 0) sector as an intermediate step. Our calculations gave a positive vertical electron affinity of 0.17 eV using electron attachment to the $1a_u$ orbital, hence indicating a possible stable anionic state. The basis set used is not, however, expected to describe anions well and this conclusion must be treated with some skepticism, although typically EAs are underestimated in *ab initio* calculations.

Tables 3 and 4 present the singlet and triplet excitation energies with the chosen model space. The trends for both the singlet and triplet states are clear. For all except two of the triplet states, the SCF excitation energies are larger than the correlated energies. The use of the Davidson correction for unlinked diagrams in the CI calculation (CISD + Q) further reduces the transition energies for all except the same two states as compared to CI. The Fock space results which rigorously eliminate all unlinked diagrams, show the same general trend but are in general substantially lower than the CI results, giving rise to a much better agreement with the experimental numbers. One state stands out in this comparison. The CI calculations of the $^3B_{1u}$ state indicates the correlated excitation energy is larger than the corresponding SCF number, whereas the Fock space coupled cluster results give the opposite result. This is an example where the single reference description breaks down completely. After analyzing the Fock space multireference wavefunction one finds that there are two equally important dominant configurations for this state resulting from the $1b_{2g} \rightarrow 2b_{3u}$ and $1b_{1g} \rightarrow 1a_u$ substitutions. A multireference description is therefore recommended, causing the CI calculations to be a poorer approximation. As a further indication of the importance of multireference effects we found that the two

**Table 3.** Vertical singlet excitation energies in eV for *s*-tetrazine. SCF geometry, DZP basis set. CISD + Q refers to a CI calculation including the Davidson correction (adiabatic excitation energies in parenthesis)

| Electronic state | SCF[a] | CISD[a] | CISD + Q[a] | FSMRCC | Experiment |
|---|---|---|---|---|---|
| $^{1}B_{3u}$<br>$3b_{3g} \rightarrow 1a_u$ | 3.78 | 3.11 | 2.89 (2.80) | 2.28 | (2.25) |
| $^{1}A_u$<br>$3b_{3g} \rightarrow 2b_{3u}$ | 5.40 | 4.46 | 4.13 | 3.44 | |
| $^{1}B_{1g}$<br>$5b_{1u} \rightarrow 1a_u$ | 7.21 | 6.24 | 5.85 | 4.98 | |
| $^{1}B_{2u}$<br>$1b_{2g} \rightarrow 1a_u$ | 7.25 | 6.71 | 6.38 (6.38) | 5.25 | (4.43–5.40) |
| $^{1}B_{2g}$<br>$4b_{2u} \rightarrow 1a_u$ | 7.89 | 7.89 | 6.72 (5.54) | 5.77 (4.80) | (3.88/4.06) |
| $^{1}A_u$<br>$6a_g \rightarrow 1a_u$ | | | | 5.83 | |
| $^{1}B_{2g}$<br>$5b_{1u} \rightarrow 2b_{3u}$ | | | | 6.29 | |
| $^{1}B_{3u}$<br>$6a_g \rightarrow 2b_{3u}$ | | | | 6.92 | |
| $^{1}B_{1g}$<br>$4b_{2u} \rightarrow 2b_{3u}$ | | | | 7.26 | |
| $^{1}B_{1u}$<br>$1b_{2g} \rightarrow 2b_{3u}$ | 8.64 | 8.27 | 8.10 | 7.91 | |
| $^{1}B_{1u}$<br>$1b_{1g} \rightarrow 1a_u$ | | | | 8.48 | |
| $^{1}B_{2u}$<br>$1b_{1g} \rightarrow 2b_{3u}$ | | | | 9.21 | |

[a] Ref. [23]

states that showed the next largest discrepancies between the CI and coupled cluster numbers, $^{3}B_{2g}$ and $^{1}B_{2u}$, were also the two other states that had substantial multireference character. Sheiner and Schaefer also investigated how the shift in equilibrium geometry of the excited states affected their transition energies and found that for all the experimentally known states only the $^{1}B_{2g}$ energy was substantially changed. Although the FSMRCC method is geared towards vertical excitation energies we performed a separate calculation for this state. As can be seen from Table 3 the adiabatic transition energy for this state is about 1 eV lower than the vertical excitation energy. Although the adiabatic calculation reduced the discrepancy between our calculation and the experimental result the difference is still substantial and further investigations are necessary for this state. In particular, its relatively high energy suggests the importance of a Rydberg character that is not well described without adding diffuse basis functions to the current basis set. For other states where experimental results are available the coupled cluster energies fair well and far better than the CI results. A further advantage of our multireference treatment is borne out by the fact that we obtained several states of the same symmetry in contrast to the CI calculation. Several of these states fall in the same energy range as the lower roots as can be seen in Tables 3 and 4.

**Table 4.** Vertical triplet excitation energies in eV for *s*-tetrazine. SCF geometry, DZP basis set. CISD + Q refers to a CI calculation including the Davidson correction (adiabatic excitation energies in parenthesis)

| Electronic state | SCF[a] | CISD[a] | CISD + Q[a] | FSMRCC | Experiment |
|---|---|---|---|---|---|
| $^3B_{3u}$<br>$3b_{3g} \rightarrow 1a_u$ | 3.09 | 2.44 | 2.23 (2.15) | 1.48 | (1.69) |
| $^3A_u$<br>$3b_{3g} \rightarrow 2b_{3u}$ | 5.11 | 4.21 | 3.89 | 3.14 | |
| $^3B_{1u}$<br>$1b_{2g} \rightarrow 2b_{3u}$ | 4.82 | 5.10 | 5.14 | 3.97 | |
| $^3B_{1g}$<br>$5b_{1u} \rightarrow 1a_u$ | 6.35 | 5.43 | 5.08 | 3.99 | |
| $^3B_{2u}$<br>$1b_{2g} \rightarrow 1a_u$ | 4.20 | 4.69 | 4.86 | 4.88 | |
| $^3B_{2g}$<br>$4b_{2u} \rightarrow 1a_u$ | 7.33 | 6.55 | 6.25 | 5.01 | |
| $^3A_u$<br>$6a_g \rightarrow 1a_u$ | | | | 5.30 | |
| $^3B_{1u}$<br>$1b_{1g} \rightarrow 1a_u$ | | | | 5.74 | |
| $^3B_{2g}$<br>$5b_{1u} \rightarrow 2b_{3u}$ | | | | 6.21 | |
| $^3B_{3u}$<br>$6a_g \rightarrow 2b_{3u}$ | | | | 6.75 | |
| $^3B_{1g}$<br>$4b_{2u} \rightarrow 2b_{3u}$ | | | | 7.22 | |
| $^3B_{2u}$<br>$1b_{1g} \rightarrow 2b_{3u}$ | | | | 7.82 | |

[a] Ref. [23]

## 4. Conclusions

We have presented a Fock space multireference coupled cluster method for incomplete model spaces in some detail. The equations for calculating ionization potentials as well as excitation energies were presented diagrammatically and some of the computational advantages of the method were emphasized. Our present application to *s*-tetrazine exemplifies how the method can successfully give several properties of a system and how due to its multireference character we obtain a large number of energy differences as well as the flexibility of describing states where a single reference description fails completely.

*Acknowledgements.* This work was supported by the United States Office of Naval Research. We appreciate a grant of computer time from the Florida Supercomputer Center.

## References

1. Čižek J (1966) Chem Phys 45:4256; (1969) Adv Chem Phys 14:35; Paldus J, Čižek J, Shavitt I (1972) Phys Rev A 5:50
2. Bartlett RJ, Purvis GD (1978) Int J Quantum Chem 14:561; (1980) Phys Scr 21:255; Bartlett RJ (1981) Ann Rev Phys Chem 32:359; Bartlett RJ (1989) J Phys Chem 93:1697

3. Cole SJ, Bartlett RJ (1987) J Chem Phys 86:873
4. Rittby M, Bartlett RJ (1988) J Phys Chem 92:3033
5. Jeziorski B, Monkhorst HJ (1981) Phys Rev A 24:1668
6. Banerjee A, Simons J (1981) Int J Quantum Chem 19:207
7. Laidig WD, Bartlett RJ (1984) Chem Phys Lett 104:424; Laidig WD, Saxe P, Bartlett RJ (1987) J Chem Phys 86:887
8. Meissner L, Kucharski SA, Bartlett RJ (1989) J Chem Phys 91:6187; Meissner L, Bartlett RJ (1990) J Chem Phys 92:561
9. Mukherjee D, Moitra RK, Mukhopadhyay A (1975) Mol Phys 30:1861; (1977) ibid 33:955; Mukhopadhyay A, Moitra RK, Mukherjee D (1979) J Phys B 12:1; Sinha D, Mukhopadhyay S, Mukherjee D (1986) Chem Phys Lett 129:369
10. Offermann R, Ey W, Kümmel H (1976) Nucl Phys A 283:399; Offermann R (1976) Nucl Phys A 273:368; Ey W (1978) Nucl Phys A 296:189
11. Lindgren I (1978) Int J Quantum Chem S 12:33
12. Kutzelnigg W, Koch S (1983) J Chem Phys 79:4315
13. Lindgren I and Mukherjee D (1987) Phys Rep 151:93
14. Mukherjee D, Pal S (1989) Adv Quantum Chem 20:292
15. Sinha D, Mukhopadhyay SK, Prasad MD, Mukherjee D (1986) Chem Phys Lett 125:213
16. Haque A, Kaldor U (1985) Chem Phys Lett 117:347; (1985) ibid 120:261; Kaldor U, Haque A (1986) Chem Phys Lett 128:45; Kaldor U (1987) J Comput Chem 8:448; (1987) J Chem Phys 87:467
17. Pal S, Rittby M, Bartlett RJ, Sinha D, Mukherjee D (1987) Chem Phys Lett 137:273; Pal S, Rittby M, Bartlett RJ (1988) J Chem Phys 88:4357; (1989) Chem Phys Lett 160:212; Rittby M, Pal S, Bartlett RJ (1989) J Chem Phys 90:3214; Watts JD, Rittby M, Bartlett RJ (1989) J Am Chem Soc 111:4155
18. Mukherjee D (1986) Chem Phys Lett 125:207
19. Mukherjee D (1979) Pramana 12:203; Haque MA, Mukherjee D (1984) J Chem Phys 80:5058
20. Lindgren I (1985) Phys Scr 32:291 32:661
21. Curtis, T, Darapsky A, Muller F (1907) Chem. Ber. 40:84
22. Koenigsberger J, Vogt K (1913) Phys. Z. 14:1269
23. Scheiner AC, Schaefer III HFJ (1987) Chem Phys 87:3539
24. von Niessen W, Kraemer WP, Diercksen GHF (1979) Chem Phys 41:113
25. Huzinaga S (1965) J Chem Phys 1293; Dunning TH (1970) ibid 53:2823